Journal of Physics: Conference Series **502** (2014) 012048 doi:10.1088/1742-6596/502/1/012048

Applications of a micro-pixel chamber (μPIC) based, time-resolved neutron imaging detector at pulsed neutron beams

J D Parker[1,6], M Harada[2], K Hattori[1], S Iwaki[1], S Kabuki[1], Y Kishimoto[1], H Kubo[1,3], S Kurosawa[1], Y Matsuoka[1], K Miuchi[4], T Mizumoto[1], H Nishimura[1], T Oku[2], T Sawano[1], T Shinohara[2], J-I Suzuki[2], A Takada[1], T Tanimori[1], K Ueno[1], M Ikeno[3,5], M Tanaka[3,5] and T Uchida[3,5]

[1] Department of Physics, Kyoto University, Kyoto 606-8502, Japan

[2] Materials and Life Science Facility Division, Japan Atomic Energy Agency, Tokai, Ibaraki 319-1195, Japan

[3] Open Source Consortium of Instrumentation (Open-It), KEK, Tsukuba, Ibaraki 305-0801, Japan

[4] Department of Physics, Kobe University, Hyogo 657-8501, Japan

[5] Institute of Particle and Nuclear Studies, KEK, Tsukuba, Ibaraki 305-0801, Japan

E-mail: jparker@cr.scphys.kyoto-u.ac.jp

Abstract. The realization of high-intensity, pulsed spallation neutron sources such as J-PARC in Japan and SNS in the US has brought time-of-flight (TOF) based neutron techniques to the fore and spurred the development of new detector technologies. When combined with high-resolution imaging, TOF-based methods become powerful tools for direct imaging of material properties, including crystal structure/internal strain, isotopic/temperature distributions, and internal and external magnetic fields. To carry out such measurements in the high-intensities and high gamma backgrounds found at spallation sources, we have developed a new time-resolved neutron imaging detector employing a micro-pattern gaseous detector known as the micro-pixel chamber (μPIC) coupled with a field-programmable-gate-array-based data acquisition system. The detector combines 100μm-level (σ) spatial and sub-μs time resolutions with low gamma sensitivity of less than 10^{-12} and a rate capability on the order of Mcps (mega-counts-per-second). Here, we demonstrate the application of our detector to TOF-based techniques with examples of Bragg-edge transmission and neutron resonance transmission imaging (with computed tomography) carried out at J-PARC. We also consider the direct imaging of magnetic fields with our detector using polarized neutrons.

Neutrons, being neutral, highly penetrating particles, have found extensive use in fields ranging from materials science, engineering/manufacturing, medical, and security applications. In particular, materials science and manufacturing applications use neutrons as a probe for non-destructive testing and to study the structure and properties of bulk materials from the millimeter to nanometer scales, helping to understand and improve the materials and technologies used in our everyday lives. Presently, the realization of next-generation, high-intensity spallation neutron sources, including at J-PARC (Japan Proton Accelerator Research Complex) and the SNS (Spallation Neutron Source) in the United States, has brought time-of-flight (TOF)-based measurement techniques to the fore and spurred the development of new detector technologies to cope with the high intensities, while the ongoing development of compact accelerator-driven neutron sources in Japan, the United States, and China promises to bring these techniques and technologies to a wide audience [1].

At such pulsed sources, we can determine the energy of each neutron by measuring the time-of-flight over a known path length. This allows direct measurement of various quantities (e.g.,

[6] Author to whom any correspondence should be addressed.

transmission, scattering angle) as a function of neutron energy and requires a detector with good time resolution (<1 μs). Furthermore, a detector that combines good time resolution with good spatial resolution (100μm-order or less), low gamma sensitivity, and high rate capability opens the door to new, powerful direct imaging techniques. The present paper considers the following such techniques:

- *Bragg-edge transmission* [2] provides direct imaging of crystal structure and internal strain. It requires good time resolution to resolve small changes in Bragg-edge positions.
- *Neutron resonance transmission imaging (NRTI)* [3] provides direct imaging of isotopic/temperature distributions and requires good time resolution to resolve narrow resonance structures.
- *Magnetic imaging* [4] utilizes polarized neutrons to provide direct imaging of internal and external magnetic fields and requires good spatial resolution for imaging small details.
- *Computed tomography (CT)* allows three-dimensional image reconstruction from a set of two-dimensional images and can be combined with NRTI and magnetic imaging. A high rate capability enables shorter measurement times.

The high-intensities and large gamma backgrounds at spallation sources place strict demands on the detector system, facilitating the need for new detectors using cutting edge technologies. Traditional detectors for high-resolution neutron imaging such as imaging plates (IP) [5] and CCD (Charge-Coupled Device) cameras [6] lack adequate time resolution (IPs record no time information at all) and, being integrating-type detectors, have no means for gamma discrimination. Scintillator-based detectors [7] provide good time resolution and decent gamma discrimination, but spatial resolution is limited to the order of a millimeter. Recently developed micro-pattern detectors such as a boron-coated stacked-GEM (Gas Electron Multiplier) detector [8], a boron-doped MCP (Micro-Channel Plate) detector [9], and our μPIC (Micro-PIxel Chamber)-based detector [10,11] have the potential to satisfy most or all of the above requirements. Of these, the μPIC detector (figure 1) is the only one that provides the combination of ultra-low gamma sensitivity and 100μm-level spatial resolution (given as the Gaussian width, σ) with the ability to cover large areas (up to 40×40 cm^2) at relatively low cost. With further development, the μPIC detector is expected to reach 50~60μm spatial resolution (similar to IPs) and significantly increased counting rates. Additionally, such micro-pattern detector systems can be made quite compact, making them equally at home at large spallation sources and compact accelerator-driven sources.

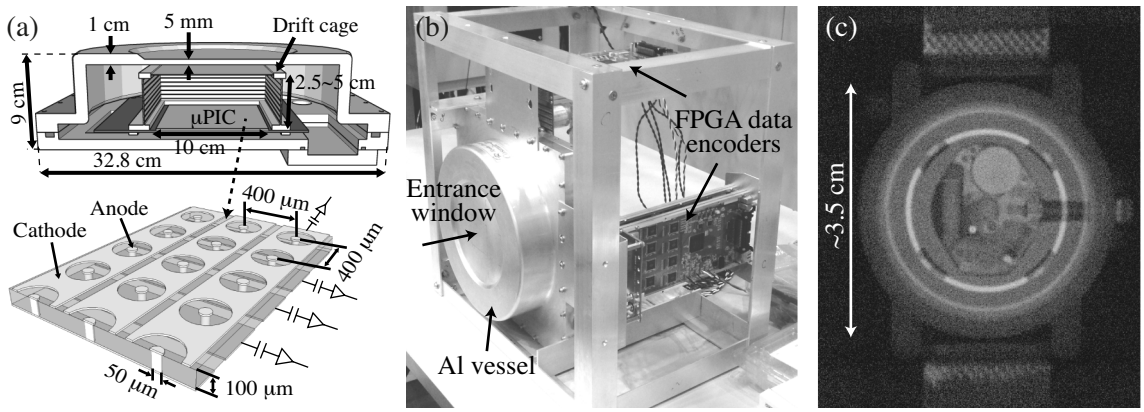

Figure 1. Schematic diagram of the μPIC detector and section of μPIC surface is shown in (a), with a photograph of the prototype detector in (b). An image of a wristwatch taken with our detector at J-PARC, NOBORU/BL10 is shown in (c). The resolution is ~120 μm (σ).

Our detector was developed under the Quantum Beam Technology Program of the Japan Ministry of Education, Culture, Sports, Science and Technology (MEXT) as part of a program to develop new detectors and technologies for the high-intensity spallation neutron source at J-PARC. The work was carried out in collaboration with members from the Japan Atomic Energy Agency (JAEA) and the High-Energy Research Organization (KEK). The prototype detector (figure 1a, b) consists of a time-projection-chamber with 2.5-cm gas depth and a 10×10-cm^2 μPIC. The μPIC [12] features a 400μm pitch with two-dimensional strip readout. Neutrons are detected via absorption on ^{3}He with 18%

efficiency at 25.3 meV using a gas mixture of Ar-C_2H_6-^{3}He (63:7:30) at 2 atm. The μPIC is coupled to a fast, FPGA (Field Programmable Gate Array)-based data acquisition system that records both the energy deposition (via time-over-threshold) and three-dimensional track (two-dimensional position plus drift time) for each neutron-induced event. This detailed tracking information allows our detector to achieve a spatial resolution of 100~120 μm (σ) and an ultra-low gamma sensitivity of $<10^{-12}$. The detector also features a time resolution of 0.6 μs and is capable of neutron rates on the order of Mcps (mega-counts-per-second) over the whole detector. The maximum count rate is achieved for a mostly homogeneous beam profile, as is typical for imaging measurements, while, due to our modular data encoder system and strip readout, the whole-detector count rate for a localized beam profile (such as encountered in small-angle neutron scattering) is reduced by at most half. Using this detector, we carried out a series of experiments at NOBORU (NeutrOn Beamline for Observation and Research Use)/BL10 at the MLF (Materials and Life Science Facility), J-PARC [13] to test detector performance and demonstrate various measurement techniques.

As an example, we used Bragg-edge transmission to make a two-dimensional map, in a single measurement, of the residual strain in a welded steel sample (figure 2a). In general, Bragg-edges appear as sudden jumps in the transmission where the neutron wavelength exceeds the Bragg-scattering condition for a given set of crystal planes. From the wavelength at the Bragg-edge, one can determine the crystal spacing ($d = \lambda/2$), and by studying the shape of the spectrum in the vicinity of the edge, one can learn about crystal properties such as grain size and texture [2]. For strain mapping, the crystal is used as a microscopic strain gauge, with the strain component derived from the deviation, in a given direction, of the crystal spacing from the unstrained value. Figure 2b shows the transmission spectra, taken with a single exposure of ~2 hours at a time-averaged neutron rate of 29 kcps, for several different regions of the 1-cm thick, double-TIG-welded 316L stainless steel sample, displaying very clear Bragg-edges with some difference between weld and steel plate regions. Figure 2c shows the estimated strain distributions for the upper and lower weld regions (indicating that the weld is under tension). Further details about this measurement and the data analysis can be found in [14].

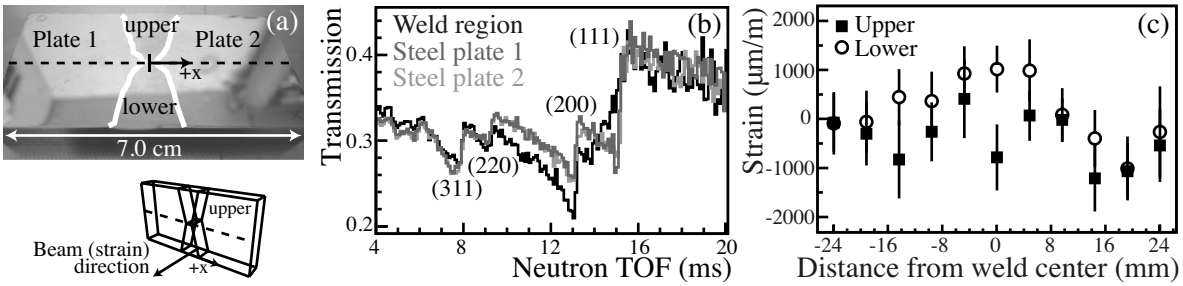

Figure 2. Strain scanning via Bragg-edge transmission. Shown here: (a) welded steel sample (white lines indicate the weld area), (b) neutron TOF spectra for weld region and steel plates (with Miller indices for some edges), and (c) longitudinal strain for upper/lower weld regions.

As another example, we combined neutron resonance transmission imaging with computed tomography. Neutron resonance techniques take advantage of the tendency of some nuclides to preferentially absorb neutrons at specific energies, unique to each nuclide, to study isotopic composition and internal temperature [3]. Resonance absorption can be directly observed by measuring the transmission, determined by taking the ratio of neutron intensities measured with and without the sample, as a function of neutron TOF. Resonances appear as sharp drops at specific energies where preferential absorption occurs. The depth of the resonance is related to the isotopic density, while Doppler-broadening of the resonance width gives information about temperature. Figure 3 shows preliminary results of a CT measurement performed at NOBORU. The sample, consisting of Cu, Mo, W, Ag, and In rods with diameters from 2 to 6 mm (figure 3a), was measured at 16 angles for ~30 minutes each (~14×10^6 neutrons per angle), with the axis of rotation aligned along the length of the rods, and images of a single CT slice were reconstructed (figures 3b—f). The indicated neutron TOF cuts, chosen to select resonances at 2039 and 579 eV (Cu), 45 eV (Mo), 19 eV (W), 5.2 eV (Ag), and 1.5 eV (In), clearly enhance the individual elements in each image. A more accurate method using fits to the known cross-sections is now under development.

Finally, we plan to apply our detector in combination with a neutron polarizing apparatus developed at J-PARC [4] to image magnetic materials with 100μm spatial resolution. Magnetic

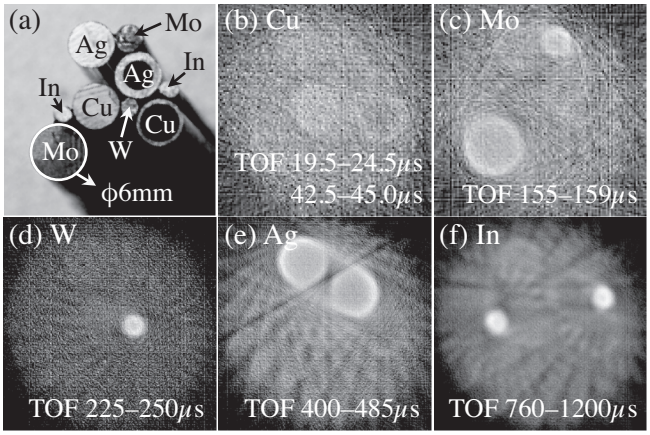

Figure 3. Resonance CT. (a) Photo of sample from above, and (b—f) computed tomography images of specific elements selected by neutron TOF (b: Cu, c: Mo, d: W, e: Ag, and f: In).

materials are at the heart of most modern technology and, in particular, emerging green technologies (e.g, electric motors for hybrid vehicles). Direct imaging of internal and external magnetic fields *in situ* with high-resolution would be an invaluable tool for the understanding and optimization of these important materials. A proposed experiment, accepted for the J-PARC/MLF 2013A run period but subsequently cancelled due to the radiation accident in May, would use this setup to image the magnetic domains in a sheet of Permalloy before and after stressing. Bragg-edge transmission would also be used to study the alterations of the crystal structure. We hope to carry out this first test experiment for magnetic imaging during in the next MLF user time.

Using high-intensity pulsed neutron sources, the combination of TOF-based measurement with high-resolution imaging produces a set of powerful techniques that allow direct imaging of bulk properties with short measurement times. Such techniques require an equally powerful and flexible detector, for which our μPIC-based detector is an excellent candidate. Additionally, although not discussed here, the application of such a high-resolution detector to small-angle neutron scattering (SANS) would provide access to small values of momentum transfer (i.e., smaller scattering angles) in a compact setup. Development and validation of our detector system, to improve spatial resolution and data rate, and of the TOF-based direct imaging techniques are ongoing.

Acknowledgments
This work was supported by the Quantum Beam Technology Program of the Japan Ministry of Education, Culture, Sports, Science, and Technology (MEXT). The neutron experiments were performed at NOBORU (BL10) of the J-PARC/MLF with the approval of the Japan Atomic Energy Agency (JAEA), Proposal No. 2009A0083.

[1] Carpenter J M 2012 *Phys. Proc.* **26** 1—7; Union for Compact Accelerator-driven Neutron Sources (UCANS) http://www.indiana.edu/~lens/UCANS/
[2] Sato H, Takada O, Iwase K, Kamiyama T and Kiyanagi Y 2010 *J. of Phys. Conf. Series* **251** 012070; Santisteban J R, Edwards L, Fizpatrick M E, Steuwer A and Withers P J 2002 *Appl. Phys.* A **74** S1433—6
[3] Sato H, Kamiyama T and Kiyanagi Y 2009 *Nucl. Instr. and Meth.* A **605** 36—9
[4] Shinohara T *et al.* 2011 *Nucl. Instr. and Meth.* A **651** 121—5
[5] Kobayashi H and Satoh M 1999 *Nucl. Instr. and Meth.* A **424** 1—8
[6] Lehmann E H, Frei G, Kühne G and Boillet P 2007 *Nucl. Instr. and Meth.* A **576** 389—96
[7] Hirota K *et al.* 2005 *Phys. Chem. Chem. Phys.* **7** 1836—8
[8] Uno S *et al.* 2012 *Phys. Proc.* **26** 142—52
[9] Tremsin A S, McPhate J B, Vallerga J V, Siegmund O H W, Feller W B, Lehmann E and Dawson M 2011 *Nucl. Instr. and Meth.* A **628** 415—8
[10] Parker J D *et al.* 2013 *Nucl. Instr. and Meth.* A **697** 23—31
[11] Parker J D *et al.* 2013 *Nucl. Instr. and Meth.* A **726** 155—61
[12] Ochi A *et al.* 2001 *Nucl. Instr. and Meth.* A **471** 264—7
[13] Maekawa F *et al.* 2009 *Nucl. Instr. and Meth.* A **600** 335—7
[14] Parker J D *et al.* 2010 *IEEE Nuclear Science Symposium Conference Record* (©2010 IEEE) pp 291—7